A Catalytically Active Membrane Reactor for Fast, Highly Exothermic, Heterogeneous Gas Reactions. A Pilot Plant Study

Jan W. Veldsink,* Geert F. Versteeg, and Wim P. M. van Swaaij

Department of Chemical Engineering, University of Twente, P.O. Box 217, 7500 AE Enschede, The Netherlands

Membrane reactors have been frequently studied because of their ability to combine chemical activity and separation properties into one device. Due to their thermal stability and mechanical strength, ceramic membranes are preferred over polymeric ones, but small transmembrane fluxes obstruct a widespread industrial use of a membrane reactor. Consequently, a bench-scale membrane reactor with a tubular, macroporous membrane (d_p = 700 nm) was developed in order to attain increased fluxes. A cooling pipe was concentrically placed inside the tubular membrane to remove heat from the membrane surface, so the present membrane reactor was suitable to conduct exothermic reactions. As a model reaction, the heterogeneous oxidation of carbon monoxide over platinum, with separated feed of carbon monoxide and oxygen, was performed in the present setup. First, the present membrane reactor was characterized by the determination of the transport parameters, structure parameters of the membrane, and the external transfer coefficients. Subsequently fluxes of the reactants and products were measured over a wide range of process conditions. Especially the influence of a transmembrane pressure difference was studied extensively. Furthermore overall conversion of carbon monoxide was measured under various process conditions, and the results were compared with the simulations of a simplified, overall reactor model. From the results of the present investigation, it could be concluded that the application of a pressure difference over the membrane turned out to be a major process control parameter. It increases the product yield and preferentially directs the fluxes toward one side of the membrane. It was shown that even for macroporous catalytic membranes substantial pressure differences are allowed without any slip of unconverted reactants through the membrane. Furthermore, high degrees of conversion were observed in the present setup, and the simulations of the overall reactor model were in reasonable agreement with the experimental data. The overall model contained no adjustable parameters. From this study, the catalytically active, ceramic membrane reactor with separated feed of reactants turned out to be highly flexible and easy to control.

1. Introduction

A membrane reactor is a special type of reactor in which a ceramic or polymeric membrane is an integral part. Both organic (polymeric) and inorganic (ceramic and metal) membranes can be used either as a separation device only or in combination with the catalyst function itself. Polymeric membranes, for instance, are used in chemical reactors in order to create large specific areas (see, e.g., Chen et al., 1992). Owing to their thermal stability, chemical resistance, and mechanical strength, ceramic membranes are often preferred over polymeric ones. Membranes can be used as a catalyst support to combine their separation properties with catalytic activity. Ceramic membranes can be distinguished in porous, such as alumina, and nonporous membranes, such as Pd alloys.

In comparison with porous membranes, nonporous membrane are highly permselective toward one of the components. Therefore, Pd-based membranes have been widely studied in dehydrogenation reactions, because hydrogen is almost exclusively transported through this type of membrane (see, among others, Shu et al., 1991). Due to the thermodynamic limited conversion of dehydrogenation reactions, a Pd membrane can be used for continuous hydrogen withdrawal from the reaction mixture in order to increase the conversion. Itoh (1987) studied the dehydrogenation of cyclohexane to benzene and used a Pd membrane as a hydrogen-permeable wall of a packed catalyst bed. It was experimentally demonstrated that the application of the Pd membrane to separate the hydrogen from the reactants resulted in an increased conversion. Many configurations and applications for Pd-based membranes were studied by Gryaznov (1992) and co-workers (e.g., Gur'yanova et al., 1988). This group also studied the concept of heat removal of an endothermic reaction by an exothermic reaction proceeding at the opposite side of the membrane and vice versa. At one side of the membrane the endothermic dehydrogenation of a hydrocarbon proceeds and the hydrogen that permeates through the membrane reacts at the opposite interface with oxygen to supply the necessary heat. However, nonporous membranes suffer from low transmembrane fluxes, and also additional problems related to metal sintering and mechanical problems obstruct a widespread use of these membranes in chemical reactors. Extensive reviews of Pd membranes in chemical reactors were presented by Shu et al. (1991) and Hsieh (1991).

Porous membranes were also studied in chemical reactors for high-temperature applications, and an overview was presented by Hsieh (1991). Usually, these membranes are made of silica and/or alumina, which have become available with well-defined and narrow pore size distributions (Leenaars et al., 1984, 1985).

* To whom correspondence should be addressed at the Department of Chemical Engineering, University of Groningen, Nijenborgh 4, 9747 AG Groningen. FAX: (+50)-634479. E-mail: veldsink@chem.rug.nl.

0888-5885/95/2634-0763$09.00/0

Zaspalis et al. (1991a,b) used asymmetric membranes with a microporous, catalytic top layer, for the methanol oxidation reaction (1991a) and the catalytic NO_x reduction with ammonia (1991b) and discussed several reactor configurations and operation modes. With the exception of the flow-through mode, the transport of reactants through the membrane was normal to the flow direction of the gas. Comparison of the different modes for the methanol oxidation showed that the flow-through mode yielded a higher methanol conversion due to a better utilization of the catalyst by methanol, but a lower selectivity toward formaldehyde (Zaspalis et al., 1991a). From Zaspalis' work it could be concluded that the catalytic membrane reactor provides for a high flexibility and good control.

In comparison with other gases, hydrogen has a high mobility, so the performance of a catalytic membrane reactor (CMR) has been frequently studied for the processing of equilibrium reactions involving hydrogen. Champagnie et al. (1992) presented an experimental study on the dehydrogenation reaction of ethane in a tubular CMR containing a multi-layer membrane with smallest pores of 40 nm—Knudsen transport prevails—and with palladium as a catalyst. Ethane mixtures were supplied to one side of the membrane and the reaction products which permeated the membrane were swept away by an inert gas. In this setup conversions above the equilibrium conversion were obtained, owing to the separation properties of the membrane, which was confirmed by model calculations.

From the aforementioned studies, it can be concluded that a suitable membrane for a CMR should have both a high permeability and a good separation selectivity. To attain increased fluxes Sloot et al. (1990, 1991, 1992) presented a nonpermselective CMR which contained a membrane with a relatively large average pore diameter, $d_p \approx 400$ nm. Moreover, the membrane in their CMR was used to provide a well-defined and controlled catalytic interface between two reactants present at opposite sides of the membrane. This concept of a nonpermselective catalytic membrane reactor with separated feed of reactants (CMRSR) was experimentally tested for the Claus desulfurization reaction and catalytic reduction of NO_x. Cini and Harold (1991) used this concept in multiphase reaction systems and demonstrated it as a suitable alternative to trickle-bed reactors because it is possible to control the liquid distribution over the catalyst and it avoids the occurrence of hot spots. Sloot et al. (1990, 1992) also presented a flux model to predict the transmembrane fluxes of reactants and products for vapor-phase reactor applications with instantaneous equilibrium reactions, and from their calculations they observed some interesting features of a CMRSR. For a sufficiently high equilibrium constant, a small reaction zone with respect to the membrane thickness appeared to be present inside the membrane. It turned out that small changes in the process conditions of either of the gas phases were compensated for by a shift of the location of this zone, resulting in a (limited) degree of self-controllability (Sloot et al., 1991). Subsequently, it was pointed out that a transmembrane pressure difference could be used to increase the fluxes and simultaneously direct the reaction products preferentially to one side of the membrane. Due to the separation of reactants, a CMRSR has a good controllability and is expected to be a promising alternative for the processing of reactions normally requiring strict stoichiometric feed ratio of reactants.

Catalytic oxidation reactions of hydrocarbons at elevated temperatures are known to proceed fast compared with the transport rates of the components, and, owing to their high exothermicity, are prone to thermal runaway and catalyst destruction. By using a CMRSR as proposed by Sloot et al. (1990, 1991, 1992) for the processing of such reactions, the reaction control may be improved, but, moreover, due to the fact that the transport rates of the reactants and products determine the conversion rate in such a CMRSR (Veldsink et al., 1992, 1993b) thermal runaway is not likely. Furthermore, the separation of the reactants avoids explosive gas mixtures, so the CMRSR can be safely operated at higher concentration levels of the reactants. However, a suitable heat-exchanging device should be present in order to conduct highly exothermic, kinetically fast, heterogeneous gas reactions in a CMRSR.

In the present study, CMRSR for the combustion of hydrocarbons is presented which can be operated at temperatures up to 750 K. The reactor configuration consists of a tubular catalytic membrane with a large average pore diameter, $d_p \approx 1\ \mu$m. Concentrically inside the membrane a cooling pipe is placed to remove heat from the membrane surface. A general applicable flux model was developed (Veldsink, 1993), which describes the transport of reactants and products through the membrane accompanied with chemical reactions of arbitrary kinetic rate equations. For a catalytic membrane reactor with separated feed of reactants (CMRSR) slip of unconverted reactants through the membrane substantially reduces the attractive features of this type of reactor. Therefore, the CMRSR possesses a limited operation window, which allows significant simplifications of the transport model (Veldsink et al., 1992). On the basis of this approximate transport model, a more complete reactor model is presented in this study to predict the overall conversion in the present CMRSR as a function of the process conditions.

In the present experimental setup, the heterogeneous combustion of carbon monoxide over platinum was performed as a model reaction. First, fluxes of the reactants and products through the membrane are presented as a function of the process conditions, both in absence or in the presence of a transmembrane pressure difference. Second, overall conversion experiments were carried out, and these results were compared with the predictions from the reactor model.

2. Theory

Fluxes through a catalytic membrane can be calculated from the differential mass balances inside the pores, combining the transport equations, such as the dusty gas model (Mason and Malinauskas, 1983) with the reaction rate equations (see Veldsink, 1993). The steady-state transport rates of components in a porous medium, accompanied with chemical reactions, is calculated from the local conservation of mass for each participating component. For a single component, i

$$0 = -\frac{1}{r}\frac{\mathrm{d}(rN_i)}{\mathrm{d}r} + R_i \ (\mathrm{mol\ m_{cat}^{-3}\ s^{-1}}) \qquad (1)$$

In eq 1, R_i represents the local consumption or production rate according to an arbitrary kinetic rate equation. This kinetic rate expression is usually determined experimentally and is an explicitly known function of the partial pressures of the components and temperature:

$$R_i = f(T, p_1, \ldots) \qquad R_{\mathrm{inert}} = 0 \qquad (2)$$

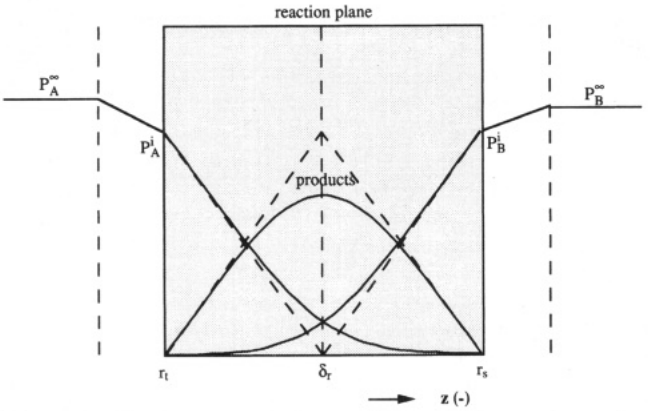

Figure 1. Typical concentration profiles over the membrane for a fast (line) and an instantaneous (dashes) reaction A + B → products.

In eq 1, N_i represents the transport flux through the membrane and should be expressed by the dusty gas model equations (see, e.g., Veldsink, 1993):

$$\sum_{j=1,j\neq i}^{n} \frac{x_i N_j - x_j N_i}{PD_{ij}^e} - \frac{N_i}{PD_{i,k}^e} = \frac{1}{RT}\frac{dx_i}{dz} + \frac{x_i}{PRT}\left(\frac{B_0 P}{\mu D_{i,k}^e} + 1\right)\frac{dP}{dz} \qquad (i = 1, ..., n) \quad (3)$$

with diffusion coefficients

$$D_{i,k}^e = \frac{4}{3}K_0\sqrt{\frac{8RT}{\pi M_i}} \qquad D_{ij}^e = \frac{\epsilon}{\tau}D_{ij}^0 \qquad (4)$$

The structure of the porous membrane is taken into account in eq 3 by three parameters, ϵ/τ, K_0, and B_0, which generally have to be determined experimentally.

At correctly chosen process conditions, slip of unconverted reactants is avoided in the CMRSR and the reactants will be completely converted inside the membrane. In the absence of a pressure difference over the membrane, typical mole fraction profiles are schematically shown in Figure 1 for a general reaction of A + B → products. Figure 1 illustrates that when the CMRSR operates in the desired regime a reaction zone exists which is smaller than the membrane thickness. Increasing the reaction rate causes a contraction of this zone and ultimately results in a reaction plane. In this case the reaction rate is infinitely fast compared with the transport rates of the reactants. It was observed from many model calculations that the transmembrane fluxes became independent of the reaction rate as soon as the reaction zone was smaller than the membrane thickness, and slip of reactants was not observable. Then the fluxes are almost completely determined by the transport rates of the reactants and products, resembling the situation of maximum enhancement in gas–liquid processes of mass transfer accompanied with chemical reactions (Veldsink et al., 1992). Owing to this phenomenon, it is possible to reduce the original transport model, presented by eqs 1 and 3.

For a binary or very diluted gas mixture, the diffusion flux of A through the membrane in the absence of both a pressure difference over the membrane and a chemical reaction, i.e., $R_i = 0$, can be derived from eqs 1 and 3:

$$N_A = \frac{-(P_A^t - P_A^s)}{RT\left(\frac{1}{k_g^t} + \frac{r_t}{r_s k_g^s} - \frac{r_t \ln(r_t/r_s)}{D_A^e}\right)} = \frac{-K_{ov}\Delta P_A}{RTr_t \ln(r_t/r_s)} \qquad (5)$$

If the reaction rate can be assumed instantaneous compared with the transport rates of the reactants, a reaction plane will exist inside the membrane, and reactants A and B (see Figure 1) cannot exist simultaneously. Provided the reaction is sufficiently fast, the calculation of the fluxes for a general reaction scheme A + υ_BB → products, with reactants A and B present at opposite sides, reduces to the calculation of the physical transport rate of each of the reactants to the reaction plane located at δ_r. Integration of eq 1 in this case leads to analogous flux expressions as eq 5 and the location of the reaction plane, δ_r, can be eliminated from the flux equations by considering that the fluxes of A and B should comply to the reaction stoichiometry. For a diluted, binary gas mixture in the absence of a transmembrane pressure difference, it is possible to derive an explicit expression for the fluxes of the reactants:

$$N_A|_{r=r_t} = -\frac{\left(D_A^e + \frac{D_B^e P_B}{\upsilon_B P_A}\right)}{(R_t + R_s + 1)}\frac{P_A}{RTr_t \ln(r_t/r_s)} \qquad (6)$$

with

$$D_A^e = \left[\frac{1}{{}^4/_3 K_0\sqrt{8RT/(\pi M_A)}} + \frac{1}{\epsilon/\tau D_A^0}\right]^{-1} \qquad (7)$$

and external mass-transfer resistances:

$$R_t = \frac{D_A^e}{k_g^t r_t \ln(r_t/r_s)}, \qquad R_s = \frac{D_B^e}{k_g^s r_s \ln(r_t/r_s)} \qquad (8)$$

In the case when the gas is not diluted and/or a pressure difference over the membrane accounts for an additional convective flow, the fluxes can be calculated from the linearized formulation of the dusty gas model equations, as suggested by Krishna (1987):

$$\sum_{j=1,j\neq i}^{n} \frac{\bar{x}_i N_j - \bar{x}_j N_i}{\bar{P}D_{ij}^e} - \frac{N_i}{\bar{P}D_{i,k}^e} = \frac{1}{RT}\frac{x_{i,\delta_r} - x_{i,r_t}}{\delta_r - r_t} + \frac{\bar{x}_i}{\bar{P}RT}\left(\frac{B_0\bar{P}}{\mu D_{i,k}^e} + 1\right)\frac{P_{\delta_r} - P_{r_t}}{\delta_r - r_t} \qquad (i = 1, ..., n) \quad (9)$$

This approximate model accurately predicted the transport through the membrane as was shown by Veldsink et al. (1993), but unfortunately, an explicit flux equation such as eq 5 cannot be obtained from this equation. However, the unknown mole fractions, inside pressure as well as the location of the reaction plane itself can be numerically solved from the flux expressions the respective mass balances. Consequently, the basis of the approximate flux model (i.e., eq 6 or 9), an overall reactor model can be developed to predict the overall conversion in a CMRSR as a function of the process conditions.

Prior to the calculations of the fluxes through the membrane, its structural parameters (B_0, K_0, ϵ/τ) should be determined experimentally from permeation mea-

surements of a pure gas through the membrane (Mason and Malinauskas, 1983). In this case the transport equation according to the dusty gas model, eq 3, reduces to

$$N_A = -\frac{1}{RT}\left(\frac{B_0 P}{\mu} + {}^4/_3 K_0 \sqrt{\frac{8RT}{\pi M_A}}\right)\frac{dP}{dz} \qquad (10)$$

For a tubular membrane with boundary conditions at $z = r_t$, $P = P_t$; $z = r_s$, $P = P_s$, and constant flux and physical parameters over the membrane eq 10 results in

$$N_{A|z=r_t} = \left(\frac{B_0(P_t + P_s)}{2\mu} + {}^4/_3 K_0 \sqrt{\frac{8RT}{\pi M_A}}\right)\frac{(P_s - P_t)}{r_t \ln(r_t/r_s)RT} \qquad (11)$$

According to (11) a plot of the ratio of the permeation flux over the transmembrane pressure difference as a function of the membrane average pressure yields a straight line. From the slope and intercept, the permeability factor, B_0, and the Knudsen factor, K_0, can be obtained, respectively. If the pores are supposed as noninterconnected, circular capillaries of radius r_p, the values of K_0 and B_0 can be directly calculated (Mason and Malinauskas, 1983) as a function of the pore radius and the tortuosity:

$$K_0 = \epsilon r_p/2\tau, \qquad B_0 = \epsilon r_p^2/8\tau \qquad (12, 13)$$

If this simple structure model holds, the value of the porosity–tortuosity ratio, ϵ/τ, can be derived from the experimental results of B_0 and K_0:

$$\epsilon/\tau = K_0^2/2B_0 \qquad (14)$$

Since it is not very likely that in porous membranes the pores are perfectly cylindrical, eq 14 must be regarded as an approximation, and the porosity–tortuosity ratio should be determined experimentally and independently from the other parameters (Veldsink, 1993).

Overall conversion of reactants in a CMRSR is the net result of a combination of several transport rates, such as internal pore transport and external gas-to-membrane transport, as well as the degree of back mixing of the gas phases in the CMRSR. To be able to describe the overall conversion in a CMRSR setup, the rates of all transport mechanisms as well as the degree of mixing of the gas phases adjacent to the membrane should be known accurately. In the present CMRSR, the gases are flowing in annular passages at opposite sides of the membrane. Under the present experimental conditions, turbulence was not to be expected so that a Poiseuille velocity profile is present, resulting in a low degree of back-mixing. However, due to the presence of the concentric cool pipe in the tubular catalytic membrane a substantial temperature gradient may exist over the tube-side annular passage, so that natural convection may affect the velocity distribution. On the combined force and natural convective flows in annular passages several investigations have been published (among others, El-Shaarawi and Sarhan, 1981, 1980; Hanzawa et al., 1986a, 1986b) and flow reversal of the fluid along the cold wall was observed under specific process conditions, especially at low *Re* (Hanzawa et al., 1986a, 1986b).

A detailed study on the effect of natural convection for the present CMRSR was presented by Veldsink (1993), and it was shown that under the present conditions the velocity distributions were fully developed and almost identical to the Poiseuille profile. In this case the effect of natural convection can be neglected and heat transfer occurs from the hot wall, membrane, to the cooling pipe by a fluid in motion with a fully developed velocity distribution. This is known as the classical Graetz problem, and heat fluxes as well as temperature distributions as a function of the axial distance from the annulus entrance are extensively tabled for annuli by Lundberg et al. (1963). Consequently, assuming that the Chilton–Colburn analogy of heat and mass transfer (Bird et al., 1960) holds the gas-to-membrane mass transfer coefficient can be calculated from the solutions of the Graetz problem as given by Lundberg et al. (1963).

In the presence of a Poiseuille profile the axial dispersion remains limited. Hence, the overall conversion of the reactants A and B can be calculated from the gas-phase mass balances assuming plug flow. At constant conditions and flow rate the average, mixing cup, the mole fraction of A can be calculated from

$$\frac{d\bar{x}_A}{dz} = \frac{N_A \cdot 2\pi r_0 RT}{\phi_v P} \qquad (15)$$

The approximate model is completed by substitution of either eq 6 or 9 for the fluxes.

3. Experimental Setup

A pilot plant of a catalytic membrane reactor was built which consisted of a tubular, alumina membrane (i.d. = 14×10^{-3} m; o.d. = 20×10^{-3} m) with an average pore size of $d_p \approx 700$ nm. Two similar membranes were available with respective lengths of, $L = 0.275$ and $L = 0.117$ m. The ceramic membrane was connected to a pair of stainless steel (AISI 321) bellows which were subsequently connected to the stainless steel reactor shell. The bellows accomplished a gastight sealing and compensated for the differences in thermal expansion between the ceramic membrane and the metal shell. The connection of the bellows to the membrane was accomplished by Velterop B.V. (Heerhugowaard, The Netherlands). Inside the tubular membrane (tube side) a concentric stainless steel cooling pipe was present (o.d. = 6×10^{-3} m) to remove the heat from the membrane surface. Thus, the membrane reactor was divided in two annular gas passages, one enclosed by the membrane and the cooling pipe (tube side, $b = 4 \times 10^{-3}$ m) the other by the membrane and the reactor shell (shell side, $b = 15 \times 10^{-3}$ m). A schematic drawing of the present membrane reactor is shown in Figure 2. The complete reactor was placed in a temperature controlled oven, which could be used either as a startup device or compensational heating during the experiments.

Inlet gas compositions were set and controlled by Brooks' thermal mass flow controllers and preheated before entering the reactor. The carbon monoxide first passed a fixed bed of copper beads (578 K) to remove any carbonylic compounds. Normally the shell and tube sides of the CMR were operated countercurrently with the tube-side gas passing down flow, although it was easy to realize other configurations. Thermocouples (K-type) were present to monitor the inlet and effluent gas temperatures, membrane temperature, and the temperature of the cooling liquid (Tamson VT4700 oil). Tube and shell side pressures were controlled by back-pressure regulators (Tescom), and the absolute pressures could be read from a digital pressure transducer

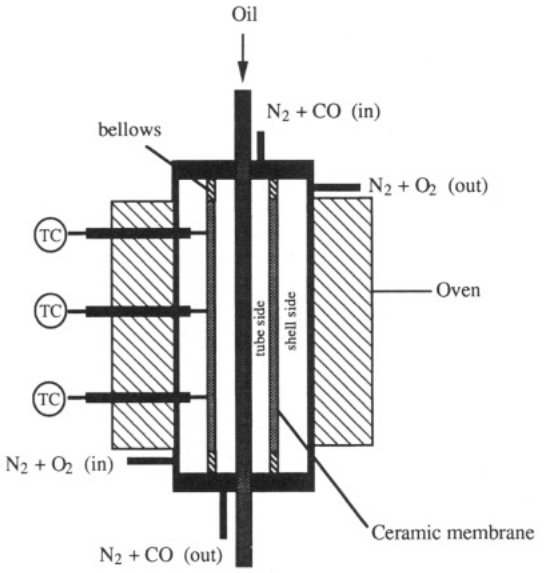

Figure 2. Schematic drawing of the pilot plant with a tubular membrane.

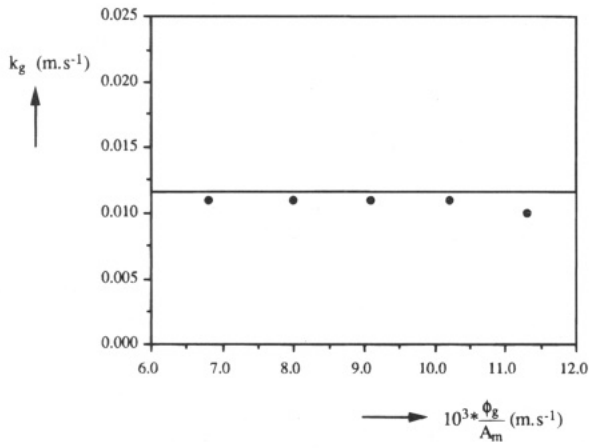

Figure 3. Gas-to-membrane mass-transfer coefficient at the tube side of the membrane plotted as a function of the gas-flow rate. Results were obtained from conversion experiments with premixed feed of oxygen and carbon monoxide at $T = 523$ K and $P = 0.2$ MPa. The line indicates the transfer coefficient from eq 16b.

(Druck, 0−0.325 MPa). Effluent gas compositions were analyzed by a CO_2 infrared analyzer (Maihak, UNOR6N, 0−2%, 0−20% vol and a gas chromatograph (Varian 3300). The gas chromatograph separated mixtures of oxygen, nitrogen, CO, and CO_2 over a Hayesep and MS 5 Å column in series. Before the effluent gas entered the analyzing section, it was mixed with a well-known flow rate of SF_6, so that the effluent flow rate could be estimated from the SF_6 concentration in the effluent gas. This method of determination avoided downstream pressure drops, which disturbed the operation conditions of the CMR. Finally, overall mass balances were satisfied within an accuracy of 15% under all process conditions.

3.1. Catalyst and Reaction. To increase the surface area, the α-Al_2O_3 tubes were first impregnated with γ-Al_2O_3 from an aqueous solution of urea and aluminum nitrate (mass ratio 1:2). Next, the membrane was heated up quickly to 373 K and dried at this temperature for 1 night. Subsequently, the nitrous compounds were removed from the surface at 473 K and the membrane was calcinated for 4 h at 673 K. Second, the membrane was impregnated with platinum from an aqueous H_2PtCl_6 solution. The impregnated membranes contained approximately 4−6% wt % γ-Al_2O_3 and 2.0−3.0% wt % Pt.

As a model reaction for the characterization of the CMRSR the heterogeneous oxidation of carbon monoxide over platinum was used:

$$CO + 0.5O_2 \rightarrow CO_2 \qquad \Delta H_r = -280 \text{ kJ mol}^{-1}$$

4. Results and Discussion

4.1. Hydrodynamics. External, gas-to-membrane mass-transfer coefficients were obtained from the solutions of the Graetz problem for annular passages as given by Lundberg et al. (1963) and by application of the Chilton−Colburn analogy of heat and mass transfer. For the present tubular membrane asymptotic values for fully developed conditions were obtained from

$$\text{shell side: } \frac{k^s_{g,A} \cdot 2b}{D^0_A} = 4.89;$$

$$\text{tube side: } \frac{k^t_{g,A} \cdot 2b}{D^0_A} = 3.52 \quad (16a,b)$$

As mentioned before, the effects of natural convection and entry length were not included in these asymptotic values, and relations 16 can, therefore, be regarded as a conservature estimation of the external mass-transfer coefficients.

Direct, experimental estimation of the external mass transfer coefficient, k_g, from conversion measurements of the heterogeneous carbon monoxide oxidation reaction is possible in the case of premixed reactants at the entrance (Veldsink, 1993). In the present CMR overall conversion of CO was measured as a function of the gas velocity in the tube side at $T = 523$ K, $P = 0.200$ MPa, in order to estimate the gas-to-membrane mass-transfer coefficient. At the tube side, inlet gas mixtures were supplied containing approximately 1.5 vol % CO and 3.2 vol % O_2, balance N_2, while pure N_2 was supplied to the shell side. Under the experimental conditions, conversion of CO ranged from 0.60 to 0.90. The overall mass-flow rates were sufficiently high to assume that natural convection did not affect the flow pattern and a Poiseuille profile was supposed to occur. The experimental results are summarised in Figure 3, plotting the tube-side k_g as a function of the actual volumetric gas-flow rate over the external membrane area, together with the results obtained from eq 16b. From Figure 3 it can be concluded that a good agreement exists between the experimentally estimated k_g and the asymptotic theoretical values as presented in eqs 16.

For the present experiments overall conversions were relatively high, and, as a result, the mass-transfer coefficients that were obtained from these experiments are very sensitive to the occurrence of axial dispersion. Furthermore, the rate of the oxidation of CO may neither be completely instantaneous nor occurring at the external membrane surface only. Owing to these uncertainties and a possible, additional contribution of natural convection, the actual value of k_g may be higher. Therefore, as mentioned before, the external mass transfer coefficient, k_g, obtained from eq 16 can be regarded as a conservative estimation.

4.2. Structure Parameters. To determine the structure parameters of the membranes, helium and nitrogen were permeated through the membrane at ambient temperature ($T = 294$ K) and at different pressures. The results were plotted in accordance with eq 11 and Figure 4 shows a typical result. The collective results are summarized in Table 1. The obtained structure parameters were not a function of the direc-

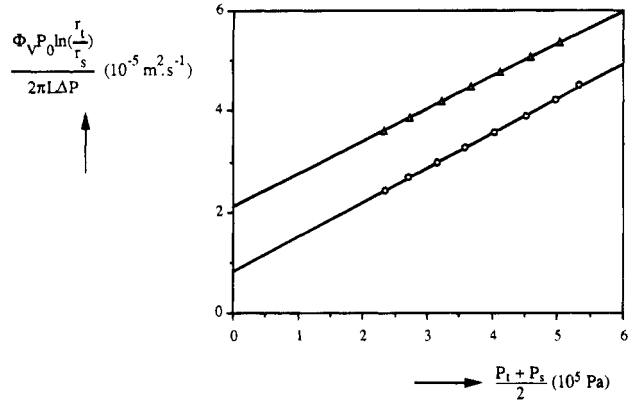

Figure 4. Permeation measurements of He and N_2 (O) through the short membrane (L = 0.117 m) plotted according to eq 11.

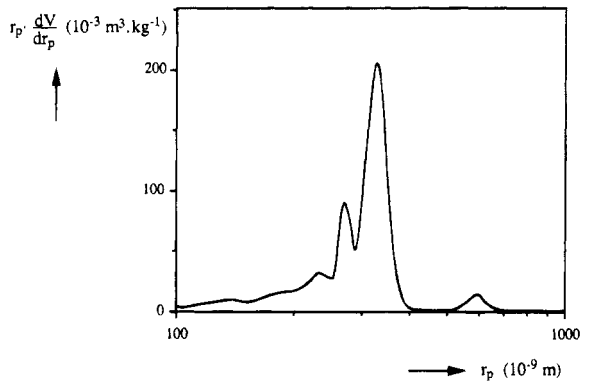

Figure 5. Mercury porosigram of the tubular membrane impregnated with Pt/γ-Al_2O_3 catalyst. The average pore radius was determined to be 250 nm.

Table 1. Structure Parameters Determined from Permeation Measurements of a Pure Gas through the Membrane (Results Summarized for Two Different Membranes)

	L = 0.275 m		L = 0.117 m	
	N_2	He	N_2	He
$10^{16} \times B_0$ (m^2)	7.721	7.989	12.13	12.48
$10^9 \times K_0$ (m)	10.535	9.385	12.53	12.53
$K_0^2/(2B_0) = \epsilon/\tau$	0.0718	0.0551	0.0784	0.0622
$10^9 \times \bar{r}_p$ (m)	293	317	344	398

tion of the gas flow, i.e., from the tube side to the shell side or vice versa. The values of the porosity–tortuosity ratio, which are also presented in Table 1 were calculated from the experimentally determined values of B_0 and K_0, by using eq 14. From eqs 12–14 also the average pore radius can be obtained and appeared to be close to the average value of the pore radius from mercury porosimetry; see Figure 5.

The ϵ/τ ratio was also obtained independently of the other structure parameters from additional diffusion experiments of CO and O_2 through the membrane. At 373 K and 0.200 MPa an inlet gas mixture of CO/N_2 (or O_2/N_2) was supplied to the tube side, while pure nitrogen was supplied to the shell side. Fluxes of CO and O_2 through the membrane have been measured and are plotted in Figure 6 as a function of the driving force in accordance with eq 5. From the results of Figure 7 the overall, transmembrane transfer coefficients of oxygen and carbon monoxide appeared to be

$$K_{CO}^{ov} = 1.17 \times 10^{-6}; \quad K_{O_2}^{ov} = 1.19 \times 10^{-6}\ (m^2/s^{-1})$$

The porosity–tortuosity ratio was calculated from eq 5. Furthermore, the continuum diffusion coefficients given

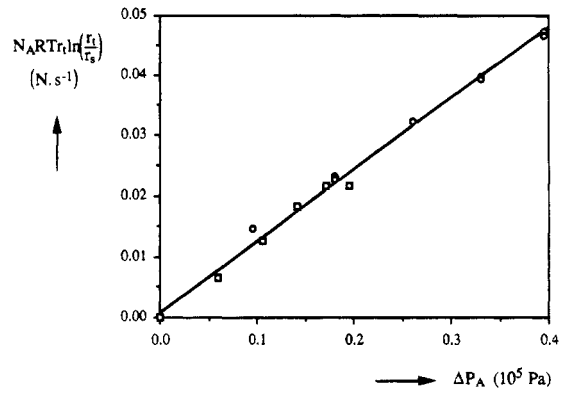

Figure 6. Diffusion of oxygen and carbon monoxide (O) through the membrane at T = 373 K and P = 0.200 MPa. Fluxes are plotted as a function of the driving force for non reaction conditions according to eq 5.

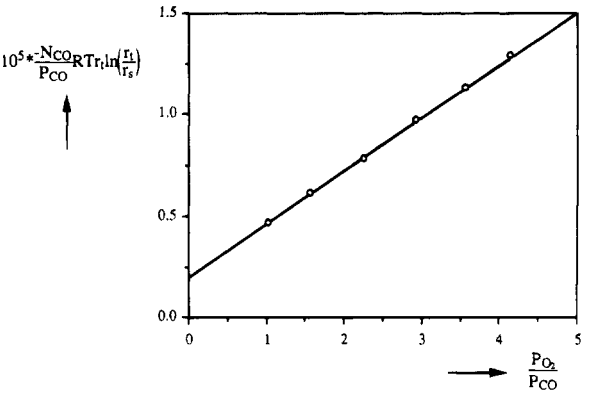

Figure 7. Plot for determining the diffusion coefficient under reaction conditions at 513 K and 0.200 MPa according to eq 6. Regression analysis resulted in values of *intercept* = 2.00×10^{-6} and *slope* = 1.32×10^{-6}, respectively.

by Marrero and Mason (1972) and an average value of K_0 from Table 1 were substituted in eq 5. The transport coefficients were calculated from eq 16, which resulted in values of ϵ/τ = 0.14 and ϵ/τ = 0.16 from the CO and O_2 diffusion, respectively. In the absence of external mass-transfer limitation the results are ϵ/τ = 0.096 and 0.10, respectively. These values are apparently higher than resulting from eq 14, as presented in Table 1, which is explained by the fact that eq 14 holds only for ideal cylindrical pores of uniform size, whereas the actual pore sizes are distributed (see Figure 5). For any distribution it can be shown that always $\bar{x}^2 \geq \bar{x}^2$ which explains the lower values in Table 1, considering eqs 12 and 13. Furthermore, it appears that the values obtained in the absence of external transport limitations are in closer agreement with the values obtained from the permeation measurements, probably indicating that the actual mass transfer coefficients are higher than calculated from eq 16.

4.3. Transport with Chemical Reaction through a Membrane. 4.3.1. Absence of a Transmembrane Pressure Difference. In a series of experiments, gas mixtures of nitrogen containing small amounts of carbon monoxide passed downflow through the tube side and diluted air countercurrently through the shell side. For these experiments a membrane with L = 0.275 m was installed in the CMRSR. At a temperature of 523 K, P = 0.200 MPa, and in the absence of a transmembrane pressure difference, CO fluxes were measured at different pressure ratios of O_2 and CO. The results were plotted in accordance with eq 6 and should yield a straight line from which the effective diffusivities of CO and O_2 could be obtained from its intercept and slope,

respectively. Since the conversions were small in these experiments, the partial pressures were assumed to be constant and equal to their logarithmic average. The results of these experiments at low partial pressures of CO are presented in Figure 7. Substitution of the values for the transfer coefficients obtained from eq 16 in eq 6 resulted in effective diffusivities of CO and O_2:

$$D^e_{CO} = 2.36 \times 10^{-6}; \quad D^e_{O_2} = 1.55 \times 10^{-6}\ (m^2\ s^{-1}) \tag{17}$$

From Marrero and Mason (1972) the continuum diffusion coefficients of O_2 and CO under the actual process conditions were obtained as

$$D^0_{N_2,CO} = 2.831 \times 10^{-5};$$

$$D^0_{N_2,O_2} = 2.747 \times 10^{-6}\ (m^2\ s^{-1})$$

at $T = 523$ K and $P = 0.2$ MPa. From eqs 7 and 17 the porosity–tortuosity ratios were determined as $\epsilon/\tau = 0.14$ from the CO and a respective value of 0.078 from the O_2 diffusivity. In the absence of mass transfer limitations the respective results for ϵ/τ are 0.11 and 0.063. For the present experiments, heat effects were not observed, and it was experimentally verified that the homogeneous oxidation reactions did not contribute to the overall conversion. The value of ϵ/τ obtained from the effective diffusivity of CO appears to be in good agreement with the results obtained from diffusion experiments in the absence of a chemical reaction, but a substantially lower value resulted from the O_2 diffusivity.

The apparent difference between the diffusivity of O_2 and CO is not readily explained, because the continuum diffusion coefficients of CO and O_2 show the same temperature dependence (Marrero and Mason, 1972), and also the Knudsen diffusivities are nearly identical. Therefore, the effective diffusion coefficients should be approximately equal in both cases. To verify the results, additional experiments of physical transport of oxygen through the membrane, analogous to section 4.2 (see Figure 6), were conducted at $T = 513$ K and $P = 0.200$ MPa. From these experiments the overall transmembrane transport coefficient (see eq 5) of oxygen appeared to be $K_{OV} = 1.72 \times 10^{-6}$ ($m^2\ s^{-1}$), which resulted in $\epsilon/\tau = 0.14$ and 0.093 in the presence and absence of external mass-transfer limitations, respectively. Within the experimental accuracy this is sufficiently close to the results from section 4.2. Therefore, the discrepancies between the diffusivities of oxygen and carbon monoxide obtained under reacting conditions from a plot of eq 6 can most likely be attributed to experimental inaccuracies.

From the present flux measurements it can be concluded that the fluxes in the present CMRSR can be accurately predicted by the approximate flux model (eq 6). The values of ϵ/τ obtained from different experiments and conditions are summarized in Table 2, and a reasonable agreement is observed between the diffusion experiments at different process conditions. The lower values resulting from the permeation experiments can be explained from the pore size distribution. Equations 16 give a reasonably accurate, although conservative, estimation of the external mass-transfer coefficient.

4.3.2. Presence of a Transmembrane Pressure Difference. The effect of a transmembrane pressure difference on the performance of a CMRSR was extensively studied theoretically by Sloot et al. (1992, 1990) and Veldsink (1993). These studies showed that the presence of a pressure difference over the membrane increases the conversion rate and directs the products toward the low-pressure side of the membrane. To verify these effects for the present reactor setup, experimental fluxes of products and reactants were determined at various pressure differences over the membrane.

Table 2. Collective Results of Porosity–Tortuosity Ratios Obtained from Different Experiments and under Different Process Conditions[a]

procedure	T (K)	with k_g (eq 16a,b)	without k_g
permeation			
N_2	294		0.075
He	294		0.059
diffusion			
CO	373	0.14	0.096
O_2	373	0.16	0.10
O_2	513	0.14	0.093
diffusion + reaction			
O_2	523	0.078	0.063
CO	523	0.14	0.11

[a] Values were calculated both in the presence and absence of external mass transfer limitations.

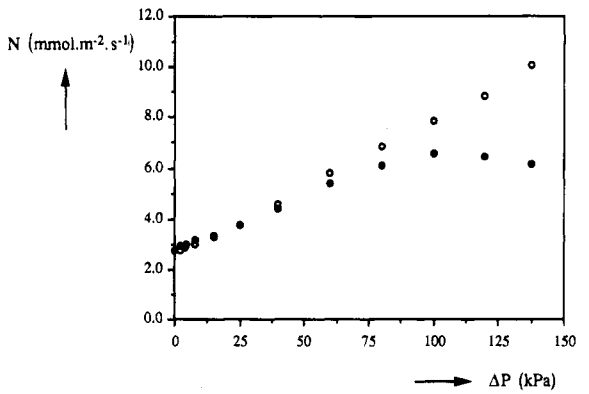

Figure 8. Reactant flux (CO, ○) and total product flux (CO_2, ●), through the membrane as a function of the transmembrane pressure difference. CO is supplied to the tube side and present at the high pressure side. Conditions: $T_m = 523$ K, $P_s = 0.20$ MPa, $P_{CO} = 13$ kPa, $P_{O_2} = 6.5$ kPa, $u^0_{g,t} = 0.58$ (m/s), $u^0_{g,s} = 0.04$ (m/s).

First the experiments were carried out at a constant shell-side pressure while the tube-side pressure was increased gradually. Consequently, the CO transport through the membrane was facilitated by the convective flow. The results are presented in Figure 8, in which both the total flux of CO through the membrane and the total outflux of CO_2 (production rate) are presented as a function of the transmembrane pressure difference. In line with the results obtained from the model calculations (Veldsink, 1993) the total CO-transport increases almost proportional with the pressure difference as a result of the contribution of the convective flow to the total transport. Initially, the CO_2 transport increases as a consequence.

The total CO_2 production, however, shows a maximum which can be explained by considering the O_2 transport, which is hindered by occurrence of the convective flow. As a result of the hindered O_2 transport and the facilitated CO transport, the reaction zone (see Figure 1) shifts toward the oxygen side of the membrane, because the transport rates of O_2 and CO should comply to the reaction stoichiometry. Consequently, O_2 has to be transported over a shorter distance to the reaction plane, which apparently compensates the effect of the convective flow, at small pressure differences over the membrane, and results in an increased CO_2 flux.

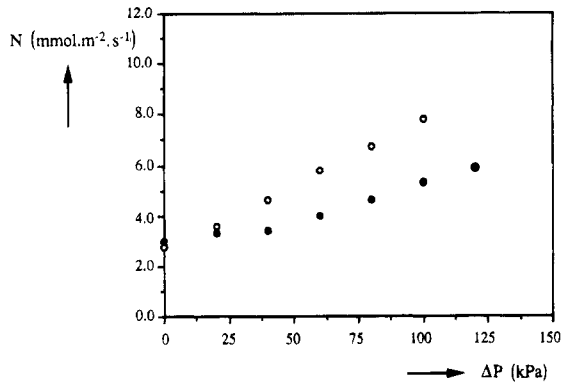

Figure 9. Reactant flux (CO, ○) and total product flux (CO_2, ●), through the membrane as a function of the transmembrane pressure difference. CO is supplied to the shell side which is the high-pressure side. Conditions: T_m = 523 K, P_t = 0.20 MPa, P_{CO} = 14 kPa, P_{O_2} = 7.5 kPa, $u^0_{g,t}$ = 0.63 (m/s), $u^0_{g,s}$ = 0.05 m/s.

However, at higher pressure differences the increase of the diffusional transport of O_2 cannot compensate for the hindrance of the opposing convective flow anymore, which causes a maximum in the CO_2 production curve. Due to the slip of unconverted reactant, the total CO flux still increases with the pressure difference. Slip of CO, albeit small (<1%), was already observed at ΔP = 60 kPa, which is just before the maximum in the CO_2 production rate curve. As a result of additional conversion at the external membrane surface, the CO_2 production rate still increases before passing through the maximum. Identical results were obtained for an exchange of the CO and oxygen feed. However, Figure 8 clearly shows that application of a transmembrane pressure difference substantially increases the production rate in a CMRSR. Moreover, transmembrane pressure differences up to approximately 50 kPa could be sustained, without slip of reactants, substantially increasing the fluxes of the reactants and the production rate.

A slightly different behavior was observed in the case when the shell-side pressure was gradually increased at a constant tube-side pressure, as shown by Figure 9. Under the presence conditions slip was already observed at ΔP = 40 kPa. Contrary to the previous results no clear maximum for the CO_2 production rate was observed for the present experimental conditions. Similar results were obtained when oxygen and carbon monoxide were exchanged. Probably the difference is caused by a different behavior of the gas volume of the shell and tube side. The tube-side external area of the membrane is smaller than at the shell side and, furthermore, the residence time of the tube side is much smaller. Another possibility might be a nonhomogeneous catalyst distribution over the membrane radius. However, these causes are only speculative, and this point of asymmetric operation is being studied at the moment.

Finally, to illustrate the remarkable effect of a pressure difference over the membrane on the direction of the product fluxes, Figure 10 presents the ratio of the experimental CO_2 fluxes to the tube and shell side of the membrane as a function of the transmembrane pressure difference. From Figure 10 it can be concluded that at the actual conditions application of a pressure difference over the membrane will direct approximately 90% of the product toward the low-pressure side of the membrane before slip of CO occurs. Figure 10 clearly demonstrates that the transmembrane pressure difference is a powerful process variable to control the direction of the reaction products.

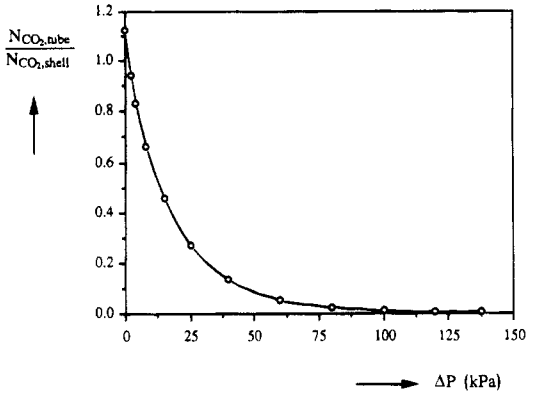

Figure 10. Ratio of the product flux to the tube side over the shell side plotted as a function of the transmembrane pressure difference. The tube-side pressure is gradually increased while the shell-side pressure remained constant. Experimental conditions as in Figure 8.

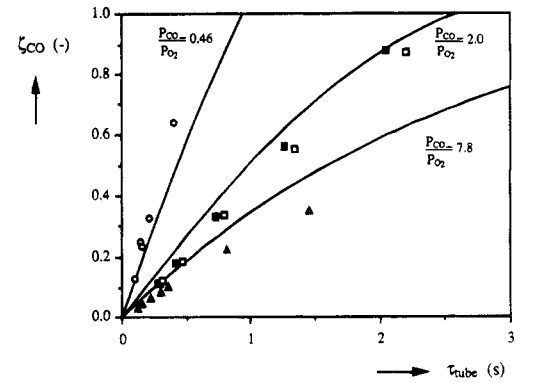

Figure 11. Overall conversion of CO in the present CMR-SFR plotted as a function of the residence time in the tube side. The lines are the results from the approximate model. Experiments were conducted countercurrently but for stoichiometric partial pressure ratio of CO and oxygen also cocurrent operation was performed (■).

4.4. Overall Conversion in a CMRSR. In the present CMRSR the overall conversion of CO that was supplied to the tube side of the membrane in these experiments was measured as a function of the average residence time in this annulus. During these experiments the shell-side conditions remained constant. The actual velocity of the gas was calculated at the average temperature between membrane and cool pipe because of the pronounced temperature difference between the membrane and cool pipe. Figure 11 presents the results of the conversion measurements as a function of the tube-side residence time in the case of a stoichiometric, sub-, or super-stoichiometric inlet partial pressure ratio of oxygen and carbon monoxide. The experimental conditions for these experiments are presented in Table 3. Normally, the operation mode of the membrane reactor was countercurrent, with downflow in the tube side, but cocurrent upflow operation of the CMRSR was also performed in the case of stoichiometric inlet partial pressure ratio of oxygen and carbon monoxide. The lines in Figure 11 represent the results from the simulations of the simplified model, given by eq 15 and flux expressions according eq 6, at conditions similar to the corresponding experiments. The structure parameters and the external mass transfer parameters have been determined either in previous experiments (see Table 1) or calculated from theory, so the present model contains no adjustable parameters.

According to the results presented in Figure 11, a CMRSR allows high degrees of conversion without slip of reactants. Furthermore simulations with the ap-

Table 3. Experimental Conditions for the Overall Conversion Experiments Presented in Figure 11[a]

	case I	case II	case III
$10^{-4} \times \Phi^0_{g,s}$ ($m^3\ s^{-1}$)	1.78	1.012	1.58
$10^{-4} \times \Phi^0_{g,t}$ ($m^3\ s^{-1}$)	0.2...2	0.1...1	0.4...1
$x^0_{O_2}$	0.010	0.109	0.013
x^0_{CO}	0.020	0.050	0.10
L (m)	0.275	0.117	0.117
T_m (K)	623	623	623
T_{cool} (K)	373	373	373
P_s (MPa)	0.200	0.200	0.200
P_t (MPa)	0.200	0.200	0.200

[a] The structure parameters of the membrane are presented in Table 1. Conditions are presented for stoichiometric (CASE I), substoichiometric (II), and superstoichiometric partial pressure ratios, respectively.

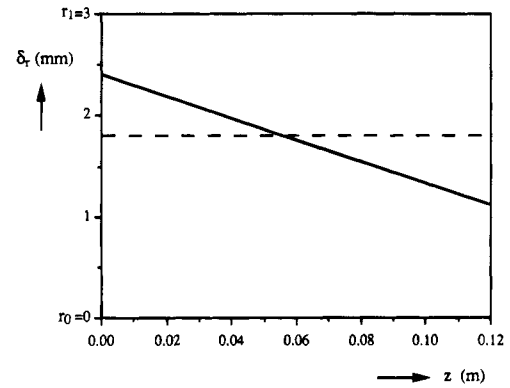

Figure 12. Location of the reaction plane as a function of the axial coordinate. Results are shown for countercurrent operation (line) and cocurrent operation (dashes). Model parameters: T_m = 623 K, $P_t = P_s = 0.20$ MPa, $x_{CO} = 0.05$, $x_{O_2} = 0.025$, $\phi_t = \phi_s = 1 \times 10^{-5}$ NM^3/s, $D^{eff}_{O_2} = 1.65 \times 10^{-6}$ m^2/s, $D^{eff}_{CO} = 2.52 \times 10^{-6}$ m^2/s.

proximate model are in reasonable agreement with the experimental results over a wide range of process conditions. Apparently the operation mode does not affect the overall conversion of CO, which is explained by the fact that the fluxes through the membrane depend on the concentration levels of both reactants at opposite sides of the membrane and, consequently, on the location of the reaction plane. For a situation of stoichiometric partial pressure ratio and equal flows of reactants A and B at the inlet (Figure 12) shows a typical plot of the location of the reaction plane as a function of the length of the membrane for both cocurrent and countercurrent operation, calculated from the approximate model. For cocurrent operation, the location of the plane is independent of the membrane length, i.e., conversion, but changes from one side of the membrane toward the other side in the case of countercurrent operation. However, the average location of this plane for countercurrent operation approximates the location of cocurrent operation, and consequently the overall conversion is almost equal for both operation modes. For the present case, cocurrent operation is preferred, because the reaction zone is located at a fixed position which avoids critical situations at the beginning or the end of the membrane.

5. Conclusions

The present study discussed a newly developed, high-temperature, nonpermselective, catalytic membrane reactor with separated feed of reactants (CMRSR). The performance of the CMRSR was demonstrated by studying the heterogeneous oxidation of carbon monoxide over supported platinum. Due to the presence of a concentric cooling pipe inside the membrane, heat can be removed from the membrane surface, without affecting the transport rates. Consequently the present CMRSR is suitable for the processing of exothermic reactions, such as combustion reactions.

In the absence of a transmembrane pressure difference the fluxes of CO and O_2 were measured at different partial pressure ratios of these reactants. From the results of these experiments it was concluded that, under the present conditions, the overall conversion rates were completely determined by the transport of the reactants. From these experiments the effective diffusivities of CO and O_2 could be determined and the results are given by eqs 17. The porosity–tortuosity ratio that resulted from these effective diffusivities appeared to be in good agreement with their values obtained from both permeation measurements and direct diffusion measurements in the absence of a chemical reaction.

It was demonstrated that, even for membrane reactors containing a macroporous membrane, substantial pressure differences over the membrane could be applied. Application of a transmembrane pressure difference favored the conversion rate and directed the reaction products toward the low-pressure side of the membrane. Increasing the pressure difference over the membrane resulted in a maximum in the production rate, which could be explained by considering the transport of the reactant moving against the convective flow.

Finally overall conversion experiments were carried out at different superficial gas velocities at the tube side of the membrane and countercurrent operation of the tube and shell side. Experiments were conducted with different partial pressure ratios of O_2 and CO, so the reaction plane inside the membrane was located differently. The results were compared with an approximated reactor model, and the results from this model appeared to be in reasonable agreement with the experimental data. Altering the operation from countercurrent into cocurrent upflow did not affect the overall conversion. The independence of the overall conversion of the operation mode could be explained from the model calculation by considering the location of the reaction plane inside the membrane as a function of the axial membrane distance.

Acknowledgment

This work would not have been possible without the financial support of GASTEC, Apeldoorn the Netherlands, which we gratefully acknowledge. We are also grateful for the contributions of J. J. Samson, S. J. ter Heide, and E. Veenendaal in the experimental part of this work. For their technical assistance we would like to thank K. van Bree and A. Schanssema.

Nomenclature

A_m = external membrane are (m_2)
$b = (r_1 - r_0)$ = gap width of the annulus (m)
B_0 = permeability constant (m_2)
d = diameter (m)
D_{ij} = binary diffusion coefficient between i and j ($m^2\ s^{-1}$)
$D_{i,k}$ = Knudsen diffusion coefficient of component i ($m^2\ s^{-1}$)
i.d. = inside diameter (m)
ΔH_r = reaction enthalpy (J mol^{-1})
k_g = gas-to-membrane mass transfer coefficient (m s^{-1})
K_0 = Knudsen constant (m)
K_{ov} = overall transport coefficient, defined by eq 5 ($m^2\ s^{-1}$)

L = length of the membrane
M = molecular mass (kg mol^{-1})
N = molar flux (mol m^{-2} s^{-1})
o.d. = outside diameter (m)
P = pressure (Pa)
P_i = partial pressure of component j (Pa)
R = universal gas constant (J mol^{-1} K^{-1})
R_s, R_t = dimensionless, external mass-transfer resistance (see eq 8)
r = radius (m)
T = temperature (K)
V = volume (m^3)
x = mole fraction
$\bar{x}$ = radical averaged mole fraction of A
z = space coordinate (m)

Greek Symbols

β = thermal expansion coefficient (K^{-1})
δ_r = location of (hypothetical) reaction plane inside the membrane (m)
ϵ = porosity
τ = tortuosity
ζ = relative conversion
μ = viscosity (Pa s)
ϱ = density (kg m^{-3})
ϕ_g = volumetric flow rate (m^3 s^{-1})

Subscripts / Superscripts

A, i, j = with respect to component A, i, or j
cool = cooling pipe
e, eff = effective
hps = high-pressure side
lps = low-pressure side
m = average
mem = membrane
p = pore
0, L = at the beginning and end of the membrane
t = tube side of the membrane
s = shell side of the membrane
0 = gas phase

Literature Cited

Bird, R. B.; Stewart, W. E.; Lightfoot, E. N. *Transport Phenomena*; Wiley: New York, 1960.

Champagnie, A. M.; Tsotsis, T. T.; Minet, R. G.; Wagner, E. The study of ethane dehydrogenation in a catalytic membrane reactor. *J. Catal.* **1992**, *134*, 713–730.

Chen, S.; Fan, H.; Kao, Y. K. A membrane reactor with two dispersion-free interfaces for homogeneous catalytic reactions. *Chem. Eng. J.* **1992**, *49*, 35–43.

Cini, P.; Harold, M. P. Experimental study of the tubular multiphase catalyst. *AIChE J.* **1991**, *37*, 997–1008.

El-Shaarawi, M. A. I.; Sarhan, A. Free convection effects on the developing laminar flow in vertical concentric annuli. *ASME J. Heat Transfer* **1980**, *102*, 617–622.

El-Shaarawi, M. A.; Sarhan, A. Developing laminar free convection in a heated vertical open-ended concentric annulus. *Ind. Eng. Chem. Fundam.* **1981**, *20*, 388–394.

Gryaznov, V. M. Platinum metals as components of catalyst-membrane systems. *Platinum Met. Rev.* **1992**, *36* (2), 70–79.

Gur'yanova, O. S.; Serov, Y. N.; Gul'yanova, S. G.; Gryaznov, V. M. Conversion of CO on membrane catalyst of Pd-Alloys. I: Reaction between CO and H2 on binary Pd-alloys with Ru and NI. *Kinet. Catal.* **1988**, *29* (4), 728–731.

Hanzawa, T.; Sako, A.; Kato, K. Velocity and temperature distributions in vertical concentric annulus with combined free and forced laminar convection. *J. Chem. Eng. Jpn.* **1986a**, *19* (2), 96–103.

Hanzawa, T.; Sako, A.; Kato, K. Combined free and forced laminar convective heat transfer from isothermally heated inner tube in vertical concentric annulus. *J. Chem. Eng. Jpn.* **1986b**, *19* (2), 96–103.

Hsieh, H. P. Catalytic membrane reactors. *Catal. Rev.-Sci. Eng.* **1991**, *33* (1 and 2), 1–70.

Itoh, N. Membrane reactors using palladium. *AIChE J.* **1987**, *33* (9), 1579–1578.

Krishna, R. A simplified procedure for the solution of the dusty gas model equations for steady-state transport in non-reacting systems. *Chem. Eng. J.* **1987**, *35*, 75–81.

Leenaars, A. F. M.; Keizer, K.; Burggraaf, A. J. The preparation and characterization of alumina membranes with ultra-fine pores. Part I: Microstructural investigations on non-supported membranes. *J. Mater. Sci.* **1984**, *19*, 1077–1088.

Leenaars, A. F. M.; Burggraaf, A. J. The preparation and characterization of alumina membranes with ultra-fine pores. Part 2: The formation of supported membranes. *J. Colloid Interface Sci.* **1985**, *105* (1), 27–40.

Lundberg, R. E.; McCuen, P. A.; Reynolds, W. C. Heat transfer in annular passages. Hydrodynamically developed laminar flow with arbitrarily prescribed wall temperatures or heat fluxes. *Int. J. Heat Mass Transfer* **1963**, *6*, 459–529.

Marrero, T. R.; Mason, E. A. Gaseous diffusion coefficients. *J. Phys. Ref. Data* **1972**, *1* (1), 3–118.

Mason, E. A.; Malinauskas, A. P. Gas transport in porous media: The dusty gas model. Elsevier: Amsterdam, 1983.

Shu, J.; Grandjean, B. P. A.; Neste, A. van; Kaliaguine, S. Catalytic palladium based membrane reactors: A Review. *Can. J. Chem. Eng.* **1991**, *69*, 1036–1060.

Sloot, H. J.; Versteeg, G. F.; van Swaaij, W. P. M. A non-permselective membrane reactor for chemical processes normally requiring strict stoichiometric feed rates of reactants. *Chem. Eng. Sci.* **1990**, *45* (8), 2415–2421.

Sloot, H. J.; Versteeg, G. F.; Smolders, C. A.; van Swaaij, W. P. M. A non-permselective membrane reactor for the selective catalytic reduction of NOx with ammonia. *Proc. 2nd int. Conf. Inorganic Membranes ICIM2-91 (Montpellier)* **1991**, 261–266.

Sloot, H. J.; Smolders, C. A.; van Swaaij, W. P. M.; Versteeg, G. F. High temperature membrane reactor for catalytic gas-solid reactions. *AIChE J.* **1992**, *38* (6), 887–900.

Veldsink, J. W. A catalytically active, non-permselective membrane reactor for kinetically fast, strong exothermic, heterogeneous reactions. Ph.D. Dissertation, University of Twente, Enschede, The Netherlands, 1993.

Veldsink, J. W.; van Damme, R. M. J.; Versteeg, G. F.; van Swaaij, W. P. M. A catalytically active membrane reactor for fast, exothermic, heterogeneous catalysed reactions. *Chem. Eng. Sci.* **1992**, *47* (9–11), 2939–2944.

Zaspalis, V. T.; van Praag, W.; Keizer, K.; van Ommen, J. G.; Ross, J. R. H.; Burggraaf, A. J. Reactions of methanol over alumina catalytically active membranes modified by silver. *Appl. Catal.* **1991a**, *74*, 235–248.

Zaspalis, V. T.; van Praag, W.; Keizer, K.; van Ommen, J. G.; Ross, J. R. H.; Burggraaf, A. J. Reactor studies using vanadia modified titania and alumina catalytically active membranes for the reduction of nitrogen oxide with ammonia. *Appl. Catal.* **1991b**, *74*, 249–260.

Received for review May 23, 1994
Revised manuscript received October 24, 1994
Accepted November 14, 1994[⊗]

IE940330Q

[⊗] Abstract published in *Advance ACS Abstracts,* February 1, 1995.